International Journal of Disaster Risk Reduction 44 (2020) 101432

Contents lists available at ScienceDirect

International Journal of Disaster Risk Reduction

journal homepage: http://www.elsevier.com/locate/ijdrr

Seismic damage scenarios for the Historic City Center of Leiria, Portugal: Analysis of the impact of different seismic retrofitting strategies on emergency planning

Elsa Anglade [a,b], Anna-Maria Giatreli [a], Anna Blyth [a], Beatrice Di Napoli [a], Francesco Parisse [a], Zahir Namourah [a], Hugo Rodrigues [c], Tiago Miguel Ferreira [a,*]

[a] ISISE-Institute for Science and Innovation for Bio-Sustainability (IB-S), Department of Civil Engineering, University of Minho, Portugal
[b] Département Génie Civil, Ecole Normal Supérieure de Paris-Saclay, France
[c] RISCO, Department of Civil Engineering, Polytechnic Institute of Leiria, Portugal

ARTICLE INFO

Keywords:
Seismic risk management
Built heritage
Masonry façade walls
Large-scale retrofitting strategies
Evacuation routes
Emergency planning

ABSTRACT

As a result of several impactful events, the focus of the international community on the effects of natural hazards in urban areas has been increasing in recent years. The framework for research and innovation on urban risk reduction and urban resilience is presently defined by several technical and societal challenges at different levels. In fact, urban risk is a very complex multi-dimensional matrix that can involve multiple elements at risk, multiple hazards, multiple temporal scales, and multiple sources of vulnerability. Understanding the impacts and interactions between these elements is an essential step towards the development of more effective risk reduction strategies, particularly in historical city centers, which, due to their characteristics, are even more demanding. Within this framework, the present paper takes advantage of a large-scale seismic vulnerability assessment method, specially developed to assess the vulnerability of masonry façade walls, to evaluate the vulnerability and to develop damage scenarios for the Historic City Center of Leiria. Based on these scenarios, obtained for the relevant seismic intensities of the region, a variety of probabilistic-based outputs related to emergency planning (inaccessible urban areas, isolated people, and possible evacuation routes) were generated and comprehensively discussed. Finally, the potential benefit resulting from the application of different seismic retrofitting strategies is also investigated, both in terms of expected damages and evacuation scenarios.

1. Introduction

The vulnerability assessment methods were developed to estimate the likelihood of the building stock suffering a particular level of damage due to an event of a specific seismic intensity. The aim is to assess the seismic vulnerability of building stock and the eventual consequences of the road block related with the building damage, and propose appropriate measures to reduce it, which is the only factor that can be modified through engineering in order to decrease the absolute seismic risk. An important asset of the vulnerability assessment methods is that they can be applied to single buildings as well as to a block of buildings and to larger-scale urban areas. The scale of application of the method is related to the amount of information collected. The larger the size of the studied area, the greater the need for more simplified but accurate and feasible approaches with fewer parameters to be evaluated, usually of an empirical nature.

Over the last years, the seismic vulnerability assessment of historical centers has been in the spotlight of several researchers, who have been developing new knowledge from large sets of damage data gathered in post-earthquake surveys. This information allowed the development and calibration of several methodologies to be applied at different scales and with distinct aims, including the large-scale risk management and mitigation. A brief overview of existing methods vulnerability assessment methods is presented, for example, in Refs. [1,2]; or in Ref. [3]; who gives an overview of the potential role played by such methods for emergency management purposes. Several methods and approaches have been recently proposed in this regard. Some of them resort to the evaluation of physical damages to support possible risk mitigation policies [4]. Some others base the analysis on more holistic approaches which consider, for example, the hazard, the vulnerability of the

* Corresponding author.
E-mail address: tmferreira@civil.uminho.pt (T.M. Ferreira).

https://doi.org/10.1016/j.ijdrr.2019.101432
Received 7 July 2019; Received in revised form 29 November 2019; Accepted 29 November 2019
Available online 30 November 2019

Table 1
Vulnerability index associated parameters classes and weights.

Parameters	Class, C_{vi}				Weight	Relative weight
	A	B	C	D	p_i	
Group 1. Geometry and Openings of the façade						
P1. The geometry of the façade	0	5	20	50	0.50	16.7/100
P2. Maximum slenderness	0	5	20	50	0.50	
P3. Area of openings	0	5	20	50	0.50	
P4. Misalignment of openings	0	5	20	50	0.50	
P5. Interaction between contiguous façades	0	5	20	50	0.25	
Group 2. Masonry materials and conservation						
P6. Quality of materials	0	5	20	50	2.00	31.5/100
P7. State of conservation	0	5	20	50	2.00	
P8. Replacement of original flooring system	0	5	20	50	0.25	
Group 3. Connection efficiency to other structural elements						
P9. Connection to orthogonal walls	0	5	20	50	2.00	33.3/100
P10. Connection to horizontal diaphragms	0	5	20	50	0.50	
P11. Impulsive nature of roofing system	0	5	20	50	2.00	
Group 4. Elements connected to the façade						
P12. Elements connected to the façade	0	5	20	50	0.50	18.5/100
P13. Improving elements	0	5	20	50	−2.00	

building environment, and other perception and capacity-related factors [5,6], or integrating the social context [7].

Considering the exposed, the present paper presents and discusses the application of a large-scale seismic vulnerability assessment approach aimed at assessing the seismic vulnerability of the façade walls of traditional masonry buildings of the Historic City Center of Leiria, Portugal. The method, an index-based formulation originally developed by Ref. [8]; is used herein to evaluate the vulnerability of the building stock as the expression of the vulnerability of the façade walls. As discussed in detail thorough the paper, the application of a methodology that considers just the seismic response of the façade wall, rather than the overall behavior of the buildings, allows developing damage scenarios, considering different seismic intensities, that can be related with the obstruction of the evacuation routes caused by the debris. In this sense, the outcoming results of the assessment are tailored to the purpose of emergency planning that is accomplished with the evaluation of inaccessible urban areas, isolated people, and possible evacuation routes. Finally, the obtained results are studied under the hypothetical application of three different seismic retrofitting techniques to consider their potential benefit, not only in terms of individual and global damages but also in terms of civil protection and urban accessibility.

2. Methodological framework

In order to clearly identify the methodological framework followed in the present work, this section presents and discusses the fundamentals of the applied seismic vulnerability assessment method, the approach adopted to characterize the historical, urban and constructive characteristics of the site, as well as the Geographic Information System tool developed to integrate, manage and visualize the information.

2.1. The vulnerability index formulation

The vulnerability index method, originally applied to buildings, was modified accordingly to consider the façade's collapse mechanisms under seismic action. The first adaptation of the original formulation of the vulnerability index was proposed by Ref. [8] based on a vast set of post-seismic damage survey data and on the identification of construction aspects that most influence the damage on masonry building façades. Later, the method was reworked and recalibrated by [9] based on both experimental fragility results and observed damages.

The façade walls, particularly of traditional masonry buildings, present many structural fragilities that affect the out of plane response when subjected to horizontal loads. This response is not always related to the global building behavior, but this is not the only reason why the independent evaluation of the façade walls' vulnerability is necessary. Observations of post-earthquake damages show that the overturning of the façade walls is one of the most concerning damage mechanisms, not only because it is commonly observed but also because of the consequences that may result from its occurrence. These consequences include direct casualties, human and economic losses, as well as obstructions to evacuation routes due to debris in the streets [1].

The method evaluates 13 parameters, associated with the seismic response of the façade walls, classified into four main groups (Table 1). These parameters are assigned to four classes, C_{vi}, of increasing vulnerability: A, B, C, and D. A numerical range corresponds to each class and a weighting factor, p_i, to each parameter that reflects its relative importance. Thus, the vulnerability index, I^*_{vf}, of the façade approach is calculated as the weighted sum of those 13 parameters and is normalized to values between 0 and 100 for ease of use, I_{vf}, shown in Equation (1).

$$I_{vf} = \sum_{i=1}^{13} c_{vi} \times p_i \quad (1)$$

2.2. Implementation of a "site approach"

According to Ref. [10]; to comprehensively characterize the site, facilitates the in-situ inspection procedure and organize the information in a systematic and logical way, the process of data collection and analysis should be based in two fundamental axes: "site context" and "building characterization". From the combination of these two axes, which are briefly described in the following paragraphs, it is possible to characterize the study site accurately and to organize it concerning different characteristics, specially selected based on the objective(s) and the scale of the analysis. Among other advantages, this process allows the buildings to be grouped with similar and singular characteristics, to identify the most vulnerable areas and to establish a spatial organization of the data.

The "site context", presented in Section 3.1, is related to the gathering of relevant information about the site. Historic city centers typically have multiple sources of information developed by different actors (e.g., governmental and management authorities, civil protection bodies, or research institutions), which, together with the several

operational management plans in force, can support the risk assessment and increase the accuracy of the analysis. Through this process, it is possible to obtain fundamental data that are difficult or impossible to obtain based on in-situ inspection.

Regarding the "building characterization", in Section 3.3, it is related to the identification of the construction techniques, materials, and architectural features shared by a group of buildings. The organization of these characteristics allows quick determination of the most vulnerable points in a specific construction typology, usually related to a historical period. Within the scope of the seismic vulnerability, the geometrical, material, and construction characteristics of the buildings, as well as their current conservation state, play a particularly important role.

2.3. Implementation of a Geographic Information System (SIG) tool

The risk assessment and mitigation in urban areas is often undertaken without the use of a comprehensive planning tool. A primary consequence of this situation is that technicians and decision-makers do not have a global view of the area under analysis, which can potentially jeopardize the effectiveness of decision-making and, in consequence, of subsequent risk mitigation measures. One of the most effective ways of tackling this issue is through the use of a multi-purpose tool connected to a relational database within a Geographic Information System (GIS) environment, from which it is possible to perform spatially integrated analysis of the building stock and manage different types of data, such as building features, survey information, seismic vulnerability and damage and loss scenarios [11]. The GIS software adopted in this study was the open-source suite [12] wherein geo-referenced graphical data (vectorized information and orthophoto maps) was combined with building parameter information. In this specific case, each polygon (corresponding to a building) was associated with several features and attributes, allowing for their visualization, selection, and searching. All of the routines used in this study were programmed within a spreadsheet environment, enabling rapid data layering and editing. Moreover, all database information associated with the GIS tool can be updated at any time, which also represents a significant added value.

3. The Historic City Center of Leiria as a case study

3.1. Site context

Leiria is a medium-size Portuguese city, situated halfway between Lisbon and Coimbra in the center of the country on the bank of the Lis River. Historically, it was of great importance since its foundation in 1135 by D. Alfonso Henriques [13] because of its strategical location for both military and commercial purposes.

The Portugal mainland is a slow seismic deforming region, leading to relatively long return periods for significant seismic events. Several studies have shown that the African and Eurasian plates' boundary has a slow convergence resulting in a series of faults. Of the recent earthquakes that occurred as a result of interaction between the plates, the Lisbon earthquake in 1755 is the largest earthquake generated offshore with a magnitude of Mw 8.5 $\pm$ 0.3 that caused major damage in the Algarve and Lisbon region and was followed by a great tsunami. During the current century, the largest earthquake recorded was on the 12th of February 2007, with a magnitude of Mw 6.1 and maximum intensities of IV-V in the city of Lisbon [14].

The Lower Tagus Valley Fault zone is the most responsible for central onshore earthquakes. The oldest one on record is the 1344 earthquake that caused severe damage in Lisbon. The largest earthquake that occurred inland during the 20th century was on the 30th of April 1909. This earthquake had an estimated magnitude of Mw 6.0–6.2 with maximum recorded intensities of IX-X and destroyed several villages, totally collapsing houses and causing recorded 46 deaths [14].

Finally, the records of the latest seismic activities during the current century report more than one hundred earthquakes with intensities equal to or larger than III on the EMS-98 macroseismic intensity scale. According to maximum intensity maps (MIM) available for the Portuguese mainland, intensity VII or VIII can be identified as representative of the seismicity of Leiria [14]. Thus, it is clear that the city is at risk of such destructive earthquakes [14].

The layout of the historic city center is centered on the *Rua Direita*, which can be considered the fundamental axis of this area with 18 streets branching perpendicularly, ten branching eastward, and eight branching westwards. The current urban configuration can be described in relation to two major landmarks: the main square and the cathedral. However, this configuration is the result of a long-term process of assembling several units with their own specific functions. The morphology and the dynamics of the urban area were affected by this process beginning in the Middle Ages between the 13th and 14th centuries, while the current layout is the result of the sprawl that occurred from the end of 19th to 20th centuries [15,16].

3.2. Study area, survey procedure and database

The vulnerability assessment work focused on the façade walls belonging to the buildings constituting the part of the city that was identified as the original historical center, which constitutes an area of approximatively 45,000 m^2. In the interest of organization, the city center was divided into three zones, separated by the main streets *Rua Barão Viamonte* and *Rua Miguel Bombarda* (Fig. 1a). The area is comprised of 232 buildings divided into three typologies according to their structural system. Reinforced concrete (RC) buildings represent 31.1% of total building stock considered; mixed structures represent 7.9%; and masonry buildings represent the majority of 61%, which is the main focus of this work. Thus, out of the 232 buildings in the study area, 71 reinforced concrete buildings were excluded from the seismic analysis. The remaining 160 buildings have one to four façades each with a total number of inspected façades equal to 251. Each façade was identified by a unique code representing the city name (LR), the zone (Z0X), the specific building number (BXXX), and the façade orientation (X).

A detailed checklist was developed to evaluate each construction characteristic of the relevant (non-reinforced concrete) façade walls, organized into the following categories: building identity and use of the building, general information, openings, layout, elements connected to the façades and also connections and damages. The checklist used for this study was adapted from a Portuguese interpretation of the Italian *Gruppo Nazionale* per *la Difesa dai Terremoti* (GNDT) checklist for seismic vulnerability evaluations of the building stock in Italy, thus combining expertise on the seismic evaluation and regional construction methods [17,18].

Information about the visible façades was documented to the extent it was observable from ground level inspections while some other necessary data were estimated on the basis of the observation of the common features across the whole façade stock. Additionally, some buildings were inspected from the interior resulting in more detailed information about the typical construction features, e. g. common types of floor slabs, common typologies of the roofing systems, inter-element connection performance, etc. Specifically, ten buildings, which correspond to 6.2% of the total buildings evaluated, were inspected from the interior. The inspected buildings and the type of inspection are shown in Fig. 1 b. Moreover, photographs taken during fieldwork were used to make assumptions about the type of masonry and the materials of the façades in case of missing information or doubts.

In order to organize the data collection, the information gathered during fieldwork was recorded in a spreadsheet database. The creation of a *parent* database with the raw collected data allowed the *child* vulnerability index tool spreadsheet to automatically pull and evaluate them with a well-constructed set of automatic functions, without needing to re-enter information manually. It was only necessary to manually enter a small amount of the information required and

Fig. 1. The division into zones (a) and the type of inspection (b).

specifically the state of conservation and the degradation pattern, which was evaluated for each single façade from the photographs taken during fieldwork.

3.3. Building characterization

The study area is composed of a fairly homogeneous building stock with common features that were easily identifiable during fieldwork. As previously mentioned, these observations were used during the vulnerability assessment procedures in order to make educated assumptions that reflected the most likely situation regarding the unknown parameters. Assumptions about the connections between orthogonal walls and between contiguous façades were made based on the appearance of the building's exterior. Details about the materials and the thickness of the walls were gained from openings in the plaster and entering the building's base floor, when possible, or in a few cases from interior inspections. For the façades analyzed, it was possible to identify some recurrent characteristics.

3.3.1. Geometrical features

The configuration of the façade walls needs to be discussed when trying to identify the typological characteristics of the building stock. Firstly, the thickness of façade walls was measured with values ranging from 0.4 m to 1.0 m with an average of 0.7 m, a range of values that is in accordance with previous studies in the same area [19]. Based on this observation, unknown thicknesses of walls were assumed equal to 0.7 m for the vulnerability assessment of the buildings.

Additionally, it can be observed that the façades' opening layouts present notable variability in the building stock. The façades facing the main streets, or the squares typically present a visible regularity in the layout (Fig. 2a), this regularity can also be seen in the dimensions of the openings, although an appreciable difference between the sizes of the openings is observed between the typical buildings and grander ones. In contrast, the secondary façades' openings do not present comparable regularity for layout nor dimensions since the doors, and the windows were generally created according to the internal plan rather than for external aesthetic purposes (Fig. 2b). Moreover, the opening layout and dimension regularity are affected by additions and interventions carried out that may have led to additional openings of differing dimensions and/or exceeding the regular grid of the existing ones (Fig. 2c).

Finally, the various non-structural elements connected to the façades are worth mentioning, since they may become debris in the streets even after low-intensity earthquakes and because they embody an additional seismic vulnerability for the façade stability. A widespread presence of large cornices was noticed on the façades facing the main streets and squares (Fig. 3a).

The building stock is additionally characterized by the presence of small stone balconies and balustrades (Fig. 3b) as well as lighter elements such as streetlamps (Fig. 3c) and air conditioning systems (Fig. 3d).

3.3.2. Materials and construction features

The evaluation of the quality of the masonry was carried out mainly through external inspections. It was observed that the façade walls are mainly comprised of stone masonry, typically locally available limestone units bonded with weak hydraulic mortar joints [19]. Observable wall sections showed (Fig. 4a and b) that façade walls are made with units of different sizes and sometimes other materials (e. g. clay bricks, marlstones, etc.) with sub-horizontal mortar joints and vertical alignment that indicates a low MQI [20]. In several cases, the presence of clay

Fig. 2. Wall facades' openings: (a) Regular layout of a principal façade wall openings facing a square; (b) irregular layout of a secondary façade wall facing a minor street; and (c) latter intervention compromising the regularity of the layout of the openings.

Fig. 3. Non-structural elements connected to the façades: (a) Cornice at the top of a building; (b) typical stone balcony, (c) light elements; (d) air conditioning systems.

brick masonry was observed to constitute the filling panels located around the façade openings. Thus, a three-leaf system was assumed consisting of poor-quality inner filling and with an absence of transversal connections (Fig. 4c). According to these observations, the most prevalent masonry was classified according to the Italian Codes [21] as "*Masonry of roughhewed stones,*" whose mechanical properties were confirmed by flat jack tests performed by Ref. [22].

Regarding the connections between structural elements, it was observed that in some cases, the presence of large cornerstones assured a good wall-to-wall connection (Fig. 5a), while when this feature was not detected a bad quality connection and improper interlocking was assumed (Fig. 5b).

Moreover, interior inspections allowed the observation of several signs of façade detachments, which were evidenced by the presence of diagonal and vertical cracks at the connecting corners of the façade walls with the internal walls (Fig. 5c). It is important to note that, in some cases, the presence of monolithic limestone posts and lintels framing of the façades' openings close to the buildings' corners can cause a detachment of the orthogonal façade compromising the connection quality between the two walls (Fig. 5d).

Fig. 4. Stone masonry with other material units (a), sub-horizontal arrangement (b) and cross-section (c) of masonry walls.

Fig. 5. Connections between structural elements: (a) Good quality connection; (b) bad quality connections between orthogonal walls); (c) detachment crack propagating in the internal corner of the façade; and (d) along the limestone lintels of the openings.

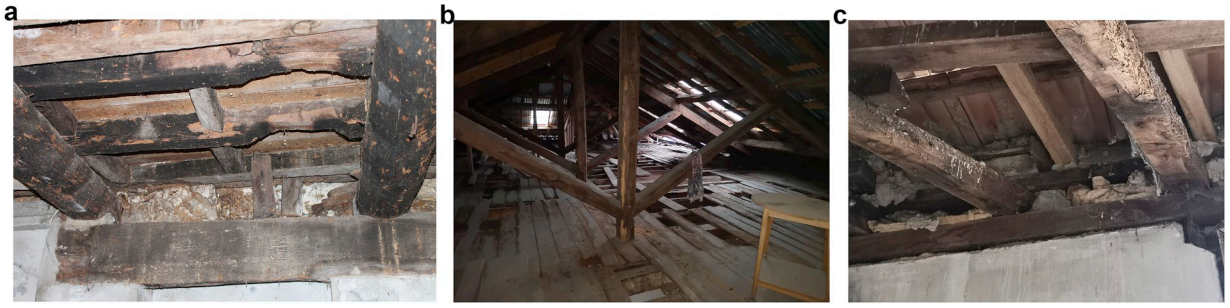

Fig. 6. (a) Example of a two-order timber floor with connection to the perimeter wall; (b) timber king post truss of a roof; and (c) mixed masonry-timber perimeter ribbon of the roof.

As shown previously in Section 2, the vulnerability of masonry façade walls is also affected by the nature of the floor slabs with which they are connected, the grade of their connection, and the impulsive nature of the roofing system of the building. In the case of the building stock of Leiria, the presence of different types of floor slabs (RC, mixed steel-concrete and timber) was observed, but the most recurrent typology was identified as timber floors connected to the supporting walls with a mortared connection or a dormant beam (Fig. 6a). Thus, the conservative assumption of the presence of flexible diaphragms with weak connections to the walls was assigned in the unknown cases. Additionally, the interior inspections allowed for the identification of a typical roofing system made with non-impulsive truss elements supporting the roof layers (Fig. 6a), connected to the perimeter walls with mixed masonry-timber repartition beams (Fig. 6c).

3.3.3. *Overall state of conservation*

A generally poor state of conservation characterizes the inspected building stock, likely due to the lack of maintenance and to deterioration processes such as chemical, physical, and biological mechanisms. The conservation state directly affects the calculation of the vulnerability index, as it is assessed by a dedicated parameter (P7). The most common pathologies of the external walls were found to be humidity, and the presence of moisture, which were observed in 49% of the building analyzed, as well as stress concentrations (42.7% of the buildings), which manifest mainly as cracks located close to openings and at the connections between façade walls. Moreover, the information collected regarding the state of conservation, expressed in a scale from 0 to 5 in the checklist and also evaluated in the post-fieldwork phase with the aid of the photographs, was used to decrease the mechanical characteristics of the masonry when the deterioration level was significant.

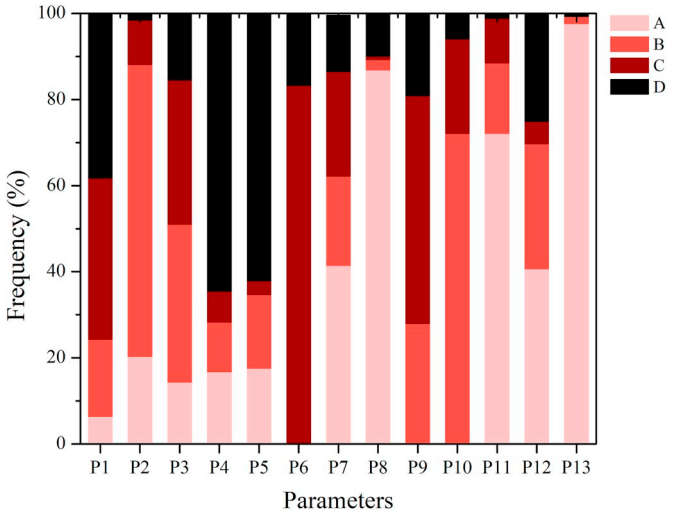

Fig. 7. Vulnerability class distribution of each one of the 13 parameters.

4. Seismic vulnerability assessment and damage scenarios

The analysis of the collected data yields the following quantitative results of the vulnerability index calculated as explained in Section 2, followed by damage distribution scenarios in terms of mean and discrete damage grades according to the EMS-98 scale [23], fragility and vulnerability curves, and collapse probabilities.

4.1. Vulnerability index results

The class distribution for all 13 parameters is shown in Fig. 7, where for each parameter is displayed the percentage distribution of the vulnerability classes. The analysis of the class distribution leads to the identification of the features that most negatively affect the vulnerability. These are the quality of materials (P6) with the totality of the façade walls in class C (82%) and D (18%), the connections between orthogonal walls (P9), with just a few (35%) walls in class B, and the connection between walls and floors (P10), with more façades scoring class B but still none in class A. It is notable that, parameters related to the geometry of the façades (P1, P4, P5) that cannot be easily modified with retrofitting, appear to have the largest percentage within class D.

The vulnerability assessment applied to the 251 façades yielded a mean seismic vulnerability index value, $I_{vf,mean}$, of 42.84. The minimum value of the vulnerability index was 16.30 and the maximum was 85.19. The associated standard deviation, σ_{Ivf}, is 12.86.

According to the I_{vf} distribution presented in Fig. 8, approximately

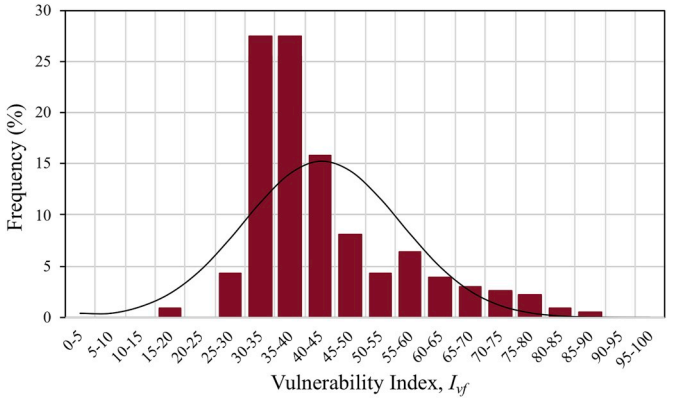

Fig. 8. Vulnerability Index distribution and comparison with the best fit normal distribution.

Fig. 9. Global vulnerability distribution of the façade walls.

70% of the façade walls have an I_{vf} value higher than 35 and 44% higher than 40, which corresponds to 175 and 111 façades, respectively; thus, 64 façades have I_{vf} values between 35 and 40. In general, 51% of the assessed façade walls have I_{vf} values in the 35–45 range, equally distributed between 35-40 and 40–45. Also, the number of façades with an I_{vf} value higher than 45 is significant, as it is around 30% of the total, representing 74 façades. The normal distribution of the sample is also plotted in Fig. 8 and compared to the actual distribution of the vulnerability index values.

Validation of the method was performed by comparing the resulting I_{vf} value with the state of conservation and the fragilities identified on-site. Indeed, the highest calculated I_{vf} values correspond to the façades with the most severe damage patterns.

The vulnerability index results were plotted with a GIS tool that allows for visualization and intuitive interpretation of the seismic assessment results. Fig. 9 presents the vulnerability map of the whole study area corresponding to the distribution of the vulnerability index values. A low I_{vf} is represented by a light color, while a higher I_{vf} is represented by a dark red color. Moreover, Fig. 10 shows that façades with I_{vf} values over 45 are present in all zones of the study area, although, in general, the higher I_{vf} values appear in the northeast area that corresponds to zone 3.

It is also important to note that the majority of the corner walls of the larger blocks have I_{vf} values over 45 in consequence of the interaction between adjacent façade walls and the aggregate position effect. The concentration of extremely vulnerable corner blocks in zone 3 can

Fig. 10. Identification of the façade walls with I_{vf} values over 45.

significantly affect the evacuation routes of this area, as illustrated in Section 5.1.

4.2. Damage distributions

4.2.1. Mean damage grades

In order to determine the damage most likely to occur for each façade under a seismic event of a given intensity, a mean damage grade μ_D was calculated according to the approach proposed by Ref. [24]. This approach was calibrated by Ref. [8] for use with the vulnerability index values calculated with the façade approach. The mean damage grade is a function of the macroseismic intensity, the vulnerability index, and a ductility factor corresponding to the type of buildings, as shown in Equation (2):

$$\mu_D = 2.51 + 2.5 \times \tanh\left(\frac{I + 5.25 \times V - 11.6}{Q}\right) \quad (2)$$

where I is the seismic hazard according to the macroseismic intensity scale defined by EMS-98 [23], V is the vulnerability index, and Q is the ductility factor. According to the calibration of [8,25]; the ductility factor Q is taken to be 2.0. The vulnerability index V was obtained according to Ref. [26] in the function of the vulnerability index I_{vf} and is expressed in Equation (3). The final values of the mean damage grade are between 0 and 5, where the higher value corresponds to the worst case, the collapse of the façade.

$$V = 0.592 + 0.0057 \times I_{vf} \quad (3)$$

The vulnerability curves plotted in Fig. 11 show the expected damage grade related to representative vulnerability index values ($I_{vf,mean}$-$2\sigma_{Ivf}$, $I_{vf,mean}$-σ_{Ivf}, $I_{vf,mean}$, $I_{vf,mean}$+σ_{Ivf}, $I_{vf,mean}$+$2\sigma_{Ivf}$), for different macroseismic intensities. The spatial distribution of the mean damage grade calculated for each façade is shown in Figs. 12 and 13, given macroseismic intensities of VII and VIII.

4.2.2. Discrete damage grades

The mean damage grade can be discretized according to the adaptation to façades of the EMS-98 damage scale [23] made by Ref. [8]. As discussed in detail by Ref. [26]; the relationship between the mean damage grade and the discrete damage grade D_k can be expressed through the damage factor, DF, present in Equation (4). In accordance with previous works addressing similar structural and construction typologies [1,8], the proposal of [27] is adopted in this work. The values that resulted from this relationship are presented in Table 2.

$$I?_D = 4\,DF^{0.45} \quad (4)$$

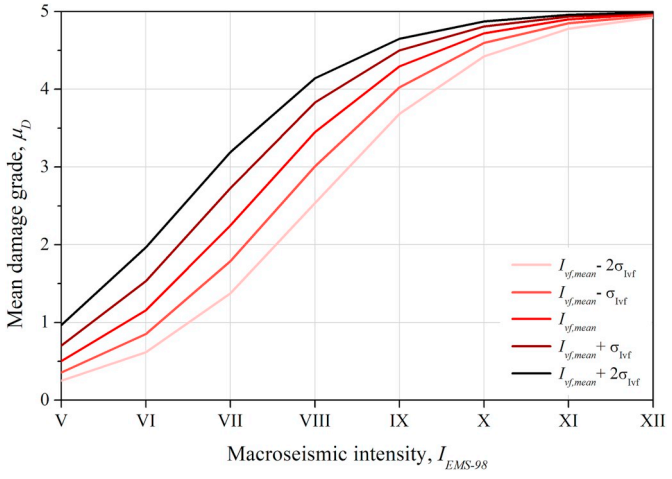

Fig. 11. Vulnerability curves obtained from the representative vulnerability index values.

Fig. 12. Damage scenario for macroseismic intensity VII.

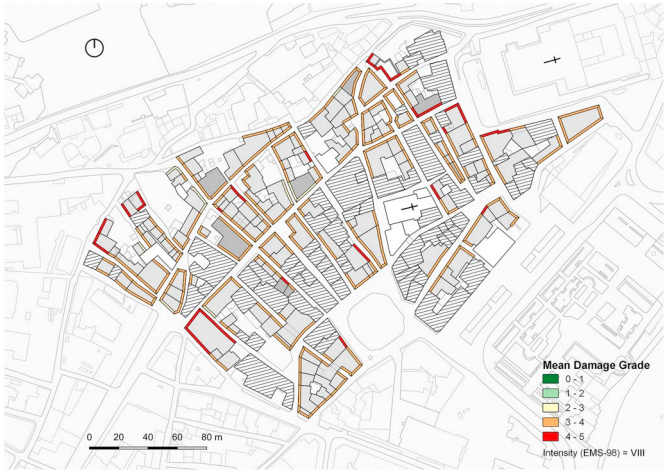

Fig. 13. Damage scenario for macroseismic intensity VIII.

Table 2
Correlation between discrete damage grade and range of mean damage grade.

Mean damage grade, μ_D	Damage factor, DF	Discrete damage grade, D_k
[0.00, 0.50]	0.00	D_0 – No damage
[0.50, 1.42]	0.01	D_1 – Slight damage
[1.42, 2.50]	0.10	D_2 – Moderate damage
[2.50, 3.50]	0.35	D_3 – Severe damage
[3.50, 4.00]	0.75	D_4 – Very severe damage
[4.00, 5.00]	1.00	D_5 - Destruction

In the case of a seismic event of intensity VII (Fig. 14a) the majority of façades (77%) would present damage grade D_2, corresponding to moderate damage [23], with few elements (~20%) having damage grade D_3, corresponding to debris in the streets. While for intensity VIII (Fig. 14b) the majority of the façades have a discrete damage grade of D_3 (71%) with the remaining cases in D_4 or D_5. With seismic events of the latter intensity, the damage of the walls and the sequential debris is significant and should be appropriately addressed in the emergency planning evaluation.

[Place here Fig. 14]

4.2.3. Fragility curves and collapse probability

An alternative method of representing damage distributions involves

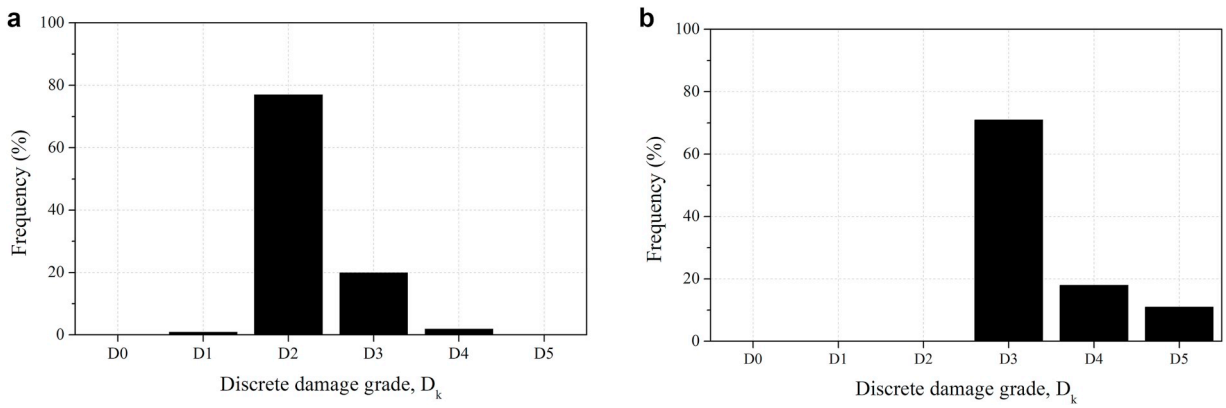

Fig. 14. Damage distribution for $I_{EMS\text{-}98}$ = VII (a) and $I_{EMS\text{-}98}$ = VIII (b).

the use of fragility curves, which enable the visualization of the probability of reaching or exceeding a certain discrete damage grade or state, D_k $(k \in [0;5])$, for a given macroseismic intensity. According to this formulation, discrete probabilities $P(D_k = d)$ can be derived from the difference of cumulative probabilities, $PD[D_k \geq d]$ applying Equation (5). As detailed in Ref. [26]; fragility curves are directly influenced by the parameters of the *beta* distribution function and allow for the estimation of damage as a continuous probability function. Thus, in accordance with [28]; *beta* distribution parameters *t*, *a*, and *b* were assumed in this work as equal to 12, 0, and 5, respectively.

$$P(D_k = d) = PD(D_k \geq d) - PD(D_{k+1} \geq d) \tag{5}$$

Knowing that, according to Table 2, damage grade D_5 corresponds to the total destruction of the façade, it is thus possible to calculate the collapse probability of a façade based on the probability of reaching this damage grade, Equation (6):

$$P_{collapse} = P(D_5) \tag{6}$$

The collapse probability curves can be seen as an alternative form of representing the vulnerability of the specific studied area in a straightforward way for an initial estimation of the severe damage probability, before further processing of the data. It is worth referring that, although this probability corresponds to a total collapse of the façade, it is possible to observe partial collapse even with the discrete damage grades D_3 and D_4, which can lead to debris in the streets and obstruction of the roads.

Fig. 15a and b shows respectively the fragility curves related to the mean vulnerability index value and the probability of collapse for the mean vulnerability index value ($I_{vf,mean}$) and lower and upper bound ranges ($I_{vf,mean}$-$2\sigma_{Ivf}$, $I_{vf,mean}$-σ_{Ivf}, $I_{vf,mean}$+σ_{Ivf}, $I_{vf,mean}$+$2\sigma_{Ivf}$).

5. Emergency planning

After an earthquake event, quickly rescuing inhabitants in the affected areas is the most crucial phase to prevent the casualties. To this end, designing appropriate prevention plans is an effective strategy to mitigate earthquake risk with regard to human, material, and economic losses. This strategy is comprised of a rescue operation plan that includes transportation of the injured, housing the homeless, and predicting physical damages. The collapse of façade walls has a direct impact on the evacuation and rescuing plans since their collapse may cause obstructions due to debris and the possibility of people being trapped in isolated areas. The identification of the most vulnerable areas constitutes a valuable resource for emergency planning. The following sections will discuss in detail how this information can lead to the definition of realistic evacuation maps and the identification of inhabitants that could become isolated [1].

5.1. Evaluation of the evacuation roads

Potentially isolated roads were identified by the presence of façades having a mean damage grade higher than 3.5 for a chosen seismic intensity of VIII, which indicates that they may be partially collapsed. Then these roads can be classified into three different typologies, according to the criteria defined by Ref. [1]:

- Road accessible by car: all façades with $\mu_D < 3.5$ and minimum free width of 4 m;
- Road accessible for pedestrian rescue: all façades with $\mu_D < 3.5$ and road width smaller than 4 m;
- Inaccessible road: façades with $\mu_D \geq 3.5$.

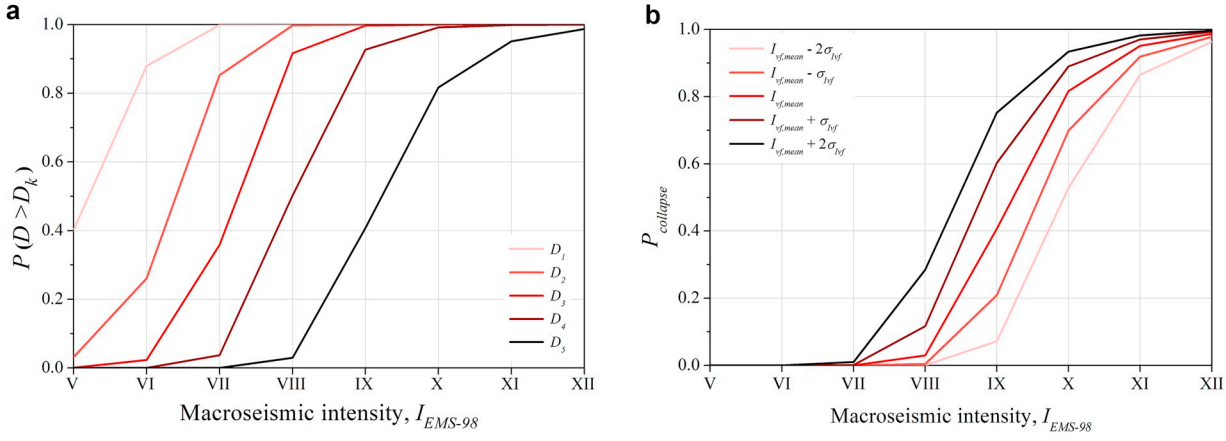

Fig. 15. Fragility curve obtained for $I_{vf,mean}$ (a) and probabilities of collapse for different vulnerability index values (b).

When compared to Ref. [1]; however, the approach followed in this work presents a relevant improvement. For the first time, the analysis relies on the consideration of each one of the building façades, contrary to what has been done in previous works where only the main façade has been considered. This represents a very significant aspect when dealing with emergency planning and urban evacuation, since the different façades of the same buildings, facing different streets, will potentially result in dissimilar levels of obstruction and inaccessibility. It is also important to highlight that although this method has not been calibrated with real data, it takes advantage of the discrete damage levels estimated for each façade, a value that was calibrated in previous works [11] resorting to real damage data.

It is worth noting that there are other methods available in the literature that could be used to define potential road blockage. For example [29], present an even simplified approach, which identifies potential road blocked based only on the building damage. On another way [30], present a detailed methodology, which was developed and calibrated from based on real damage data, that can be applied not only to estimate the amount of debris on the streets but also to compute available space for evacuees' emergency motion along paths. Less related to the building damage [31,32], proposed and integrate road closure probability scores for large-scale earthquake scenarios.

Fig. 16 illustrates the results obtained for an earthquake of intensity $I_{EMS\text{-}98}$ = VIII. The three road accessibility levels defined previously are represented as follows: green in case of vehicle accessibility, orange for pedestrian accessibility, and red when the road is blocked. The façades with a mean damage grade higher than 3.5 are represented by a dark red color. Since the streets of the city center are generally narrow, having a width lower than 4 m, the majority of the evaluated roads fall into the second or third categories, with the exception of the peripheric roads. The post-seismic scenario indicates that many blocks may be isolated, making rescue operations more difficult.

5.2. Identification of potentially inaccessible urban areas

The isolated urban areas can be identified using the results of the evacuation roads. A building is considered isolated if one of its façades is located between two façades with a mean damage grade higher than 3.5, while a block is considered isolated when all its boundary roads are inaccessible. Fig. 17 shows the eight inaccessible areas, of which five are part of a large isolated area that has been divided for the scope of the present study.

Moreover, it is possible to determine the probability of each of the identified areas being inaccessible for different seismic intensities by considering the probability of collapse of the façade responsible for the

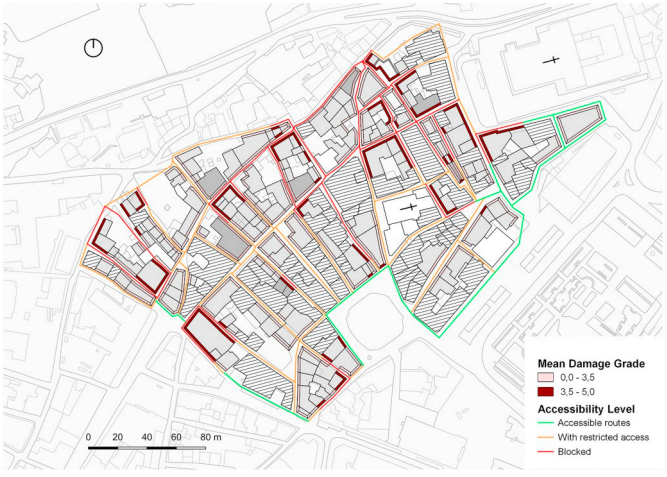

Fig. 16. Definition of evacuation routes for an earthquake scenario of $I_{EMS\text{-}98}$ = VIII.

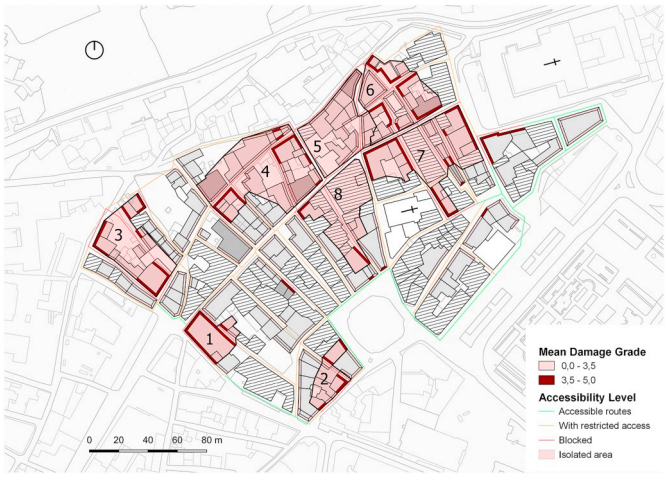

Fig. 17. Definition of the possible inaccessible areas.

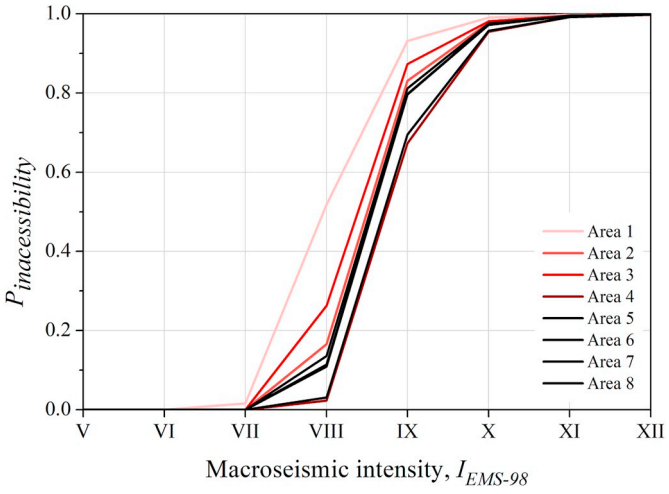

Fig. 18. Probability of inaccessibility associated with each one of the eight areas identified.

isolation of the area. According to Equation (7), the probability of inaccessibility of an area is directly related to the probability of each of the façade walls described earlier reaching discrete damage grade D_4, corresponding to $\mu_D \geq 3.5$:

$$P_{inaccessibility}(A_i) = P(D_4|F_1) \times P(D_4|F_2) \times \ldots \times P(D_4|F_n) \quad (7)$$

The probability of inaccessibility of each area in the function of the macroseismic intensity is plotted in Fig. 18.

5.3. Estimation of potentially isolated people

Emergency planning requires reliable information about the number of permanent residents in the city center but should also take into account the presence of commuters and even tourists to obtain more accurate results. Since the presence of this impermanent population can vary greatly depending on the day of week and hour of the day, the following results are based just on the permanent number of inhabitants. According to a socio-demographic census carried out by the municipality of Leiria, there are 315 residents in the area under investigation [33]. This information was refined during the inspections with additional data about the use of the buildings per floor. In some cases, the external inspection of the building was sufficient to identify unoccupied, commercial, or residential buildings. This data was used to estimate more accurately where the occupied buildings are located as well as the

Table 3
Number of people living in the isolated areas for an earthquake scenario of $I_{EMS\text{-}98}$ = VIII.

Isolated area	1	2	3	4	5	6	7	8	Total
No. Residents	7	1	3	16	27	14	4	31	103 (32.6%)
No. Potentially Isolated People	4	0	1	0	1	2	0	4	12 (3.8%)

Total number of inhabitants: 315

potential for isolated people after a given seismic event.

Based on the above information, the number of people within an isolated area is known, and the total number of potentially isolated people can be obtained by multiplying the number of residents with the probability of inaccessibility of each area [1], Equation (8):

$$N_{isolated\ people}(A_i) = P_{inaccessibility}(A_i) \times N_{residents}(A_i) \quad (8)$$

Table 3 provides the number of inhabitants for each of the eight areas identified as inaccessible in the case of an earthquake of intensity VIII and the number of potentially isolated people. In this case, almost one-third of the people living in the city center live in a critical area.

5.4. Evacuation routes and gathering areas

The definition of the evacuation routes for non-isolated people is a critical part of emergency planning that should follow the definition of the inaccessible areas in order to prevent undesirable phenomena caused by disorderly evacuation. Combining the identification of the possible evacuation routes with demographic data and the analysis of the isolated residents, it is possible to determine the number of people that could reach specified gathering areas and to evaluate the capability of these areas to host evacuees.

The gathering areas are defined according to the geometric characteristics that render these areas safe. Those characteristics are the available open space, the distance from the closest buildings, the height of those buildings, and the proximity to the main roads or highways.

The next step is the definition of the route that people should follow in their attempt to reach the gathering areas. The GIS tool was used for visualization of the results, and the map of the evacuation routes is shown in Fig. 19. The gathering areas are represented by a striped area of different colors, and the evacuation of residents to a specific gathering area is represented by arrows of the corresponding color. The optimal paths were defined based on the distance from the gathering areas and the path's tortuosity. If two ideal paths could be identified for the same block, the population of the block was equally distributed to both paths marked in the figure. During this process, it becomes clear that the vulnerability of the façade walls of corner buildings has a significant impact on the definition of the evacuation routes. Their location is critical, being the collecting point of multiple roads. Thus, the collapse of a single facade may block multiple accesses. It is notable that access to rescue Areas 1 and 4 from the southeast side is limited by collapsed or extremely damaged façade walls. The installation of signs designating the appropriate path and alternative routes is highly recommended, especially in the case of rescue Area 4, the old city's cathedral yard, which is probably the most recognized open space area by both residents and tourists.

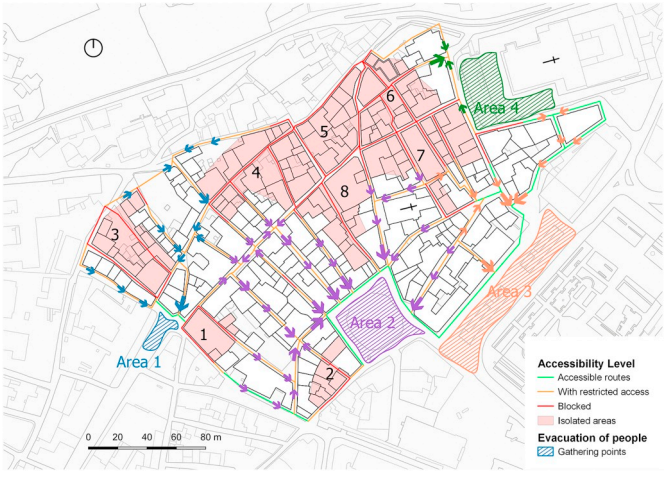

Fig. 19. Evacuation planning of the historical city center of Leiria after an earthquake of intensity $I_{EMS\text{-}98}$ = VIII.

Once those paths are identified, the number of non-isolated people that would try to reach the gathering areas is defined as the total number of inhabitants of each block, not considering those identified as isolated. In the case of an earthquake of intensity VIII, this number was divided into each possible path, and the total number of people per gathering area was calculated. According to Ref. [3], the overcrowded values for the gathering areas can be considered as more than three people per square meter, which corresponds to 0.3–0.4 m^2 for each person. The more conservative value of 0.4 m^2 per person was used in this study for the calculation of the minimum required area per person. The total number of people, the minimum required area according to this number of people, and the total occupiable area are shown in Table 4 for all four gathering areas. It is recommended that further study be carried out in order to estimate the number of non-permanent people that could be expected in the historical center. It can also be concluded that for the specific case studied, efforts should be focused on the rescuing procedure.

The rescuing procedure can be developed considering the isolated areas and the population living in each of them. It is important to prioritize rescue in areas where young children and elderly people are living. Table 5 presents the number of children and elderly people per isolated area. Areas 4, 5, 6, and 8 have the largest concentration of these demographics. They are also the areas with the greatest number of inhabitants.

According to the previous observations and the proximity of area 8 to the gathering area 2, this area is defined as the first place of intervention after an earthquake. After the evacuation of this area, the areas 4 and 5 are accessible to the civil protection bodies.

6. Seismic retrofitting strategies

6.1. Description of the retrofitting applied

The retrofitting techniques selected focus on the improvement of the façade wall connections with other structural elements. The impact of the proposed retrofitting strategies will be calculated by an updated vulnerability index after the three following techniques [1] will be applied to the buildings that have a mean damage grade higher than 3.5 for a seismic intensity of VIII:

- RS1: improvement of the wall-to-wall connections through effective tying of walls together with steel tie rods. This technique will improve parameter P9 of the I_{vf}, which evaluates the connection

Table 4
Number of people, required area and occupiable area per gathering point, considering an earthquake scenario of $I_{EMS\text{-}98}$ = VIII.

Gathering Area	Number of people	Min Area required (m^2)	Area (m^2)	Occupiable area (%)
1	30	12.0	453.5	2.7
2	129	51.6	1069.1	4.8
3	41	16.4	2034.0	0.8
4	12	4.8	1269.0	0.4

Table 5
Number of dependent people per vulnerable area.

Area	1	2	3	4	5	6	7	8	Total
No. of children and elderly people	1	1	1	6	8	6	1	11	36 (35.0%)
Total no. of people	7	1	3	16	27	14	4	31	103 (100%)

Total number of people in vulnerable areas: 103.

Fig. 20. Façades with I_{vf} over 45, after retrofitting.

between the façade and the orthogonal walls and the parameter P7, which evaluates the state of conservation of the façade.

- RS2: improvement of the wall-to-floor connections utilizing steel angle brackets anchored to walls with steel connectors and anchor plates. This technique will improve parameter P10 of the I_v, which evaluates the connection between the façade and the horizontal diaphragm.
- RS3: improvement of the wall-to-roof connection and resistance of horizontal thrusts in the event of an earthquake by means of introducing steel tie rods underneath the ceiling joints. This technique will improve parameter P11, which evaluates the impulsive nature of the roofing system.

6.2. Impact on the vulnerability

A preliminary study on the impact of the retrofitting strategy was performed considering the new vulnerability index values. Fig. 20 shows the façades with a vulnerability index higher than 45 after the application of the retrofitting. The vulnerability of the façades in the city center is noticeably decreased with a decrement of 20% of the façades presenting a vulnerability index higher than 45, going from 22% to less than 2% after the retrofitting.

After the consideration of the seismic retrofitting strategies, both mean vulnerability index values and corresponding standard deviations decrease. The mean value of the seismic vulnerability index, I_v, decreases from 42.84 to 34.77 (18.8%) with an even higher reduction of the standard deviation from 12.86 to 5.39 (58.1%). Thus, the I_{vf} distribution is less spread out, and most of the façades have values close to the mean value. The updated mean I_{vf} value is lower than the threshold value of $I_{vf} \geq 45$, considered as the maximum value above which collapse of the wall or debris in the streets is expected, according to the Iv_f -MDG-DDG correlations [1].

6.3. Impact on emergency planning

After applying the retrofitting strategy to the applicable buildings,

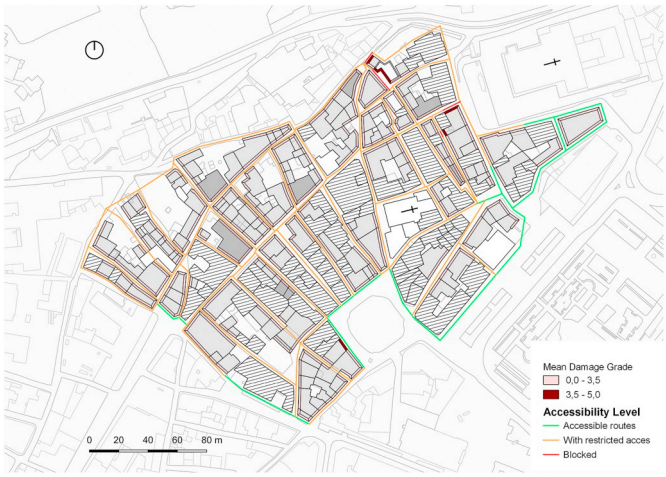

Fig. 21. Definition of evacuation routes for an earthquake scenario of $I_{EMS\text{-}98}$ = VIII after retrofitting.

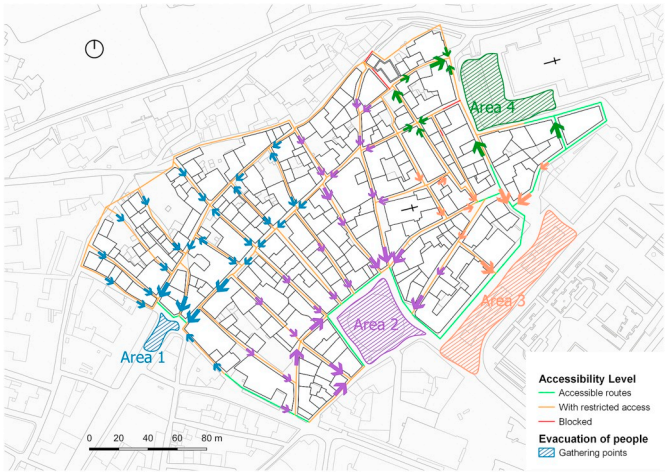

Fig. 22. Possible evacuation flow after an earthquake of intensity $I_{EMS\text{-}98}$ = VIII after retrofitting.

shown in Fig. 21, only four buildings have a façade with a damage grade higher than 3.5. Thus, almost all the roads are accessible by pedestrians after an earthquake event. Only the people living inside the few buildings with damage grades higher than 3.5 might be isolated. By looking at the data recorded during the fieldwork, it was observed that all of these buildings are currently unusable, which means that no people will be isolated after the retrofitting. These results may have a significant impact on the organization of the evacuation of the city center, as all the inhabitants are able to join a gathering point.

The definition of the evacuees' flow after retrofitting is illustrated in Fig. 22, where it can be seen that only two streets are blocked in Zone 3, near the cathedral, affecting the evacuation paths of the nearest blocks. The rest of the streets are free of debris, and the possible evacuation

Table 6
Number of people, required area and occupiable area per gathering point, after retrofitting and considering an intensity $I_{EMS\text{-}98}$ = VIII.

Gathering Area	Number of people	Min. Area required (m^2)	Area (m^2)	Occupiable area (%)
Area 1	76	30.4	453.56	6.7
Area 2	169	67.6	1069.13	6.3
Area 3	37	14.8	2034	0.7
Area 4	33	13.2	1269	1.0

Total number of people: 315.

paths are redefined according to the same criteria described for the non-retrofitting scenario.

Since there are no isolated areas or people, the number of people trying to reach the gathering points is recalculated, and the updated number of people, the minimum required area and the occupiable area per gathering point is shown in Table 6. Although the percentage of the occupiable area increases after retrofitting, it remains low, and still, the gathering areas are adequate to host the evacuees of the historical city center, in case of an earthquake of intensity VIII. It is important to notice that the evacuation paths represent the recommended path in order to have the best repartition of people in all the gathering points. In a real emergency situation, the evacuation of the population might be different as the residents might not be aware of all the possible gathering point.

7. Final comments

The vulnerability assessment method applied to the 251 façades of traditional masonry buildings of the historical city center of Leiria has shown that the most vulnerable parameters that affect the seismic response of façade walls were linked to their geometry and connections with other structural elements. The expected level of damage for the façade stock is significant for the reference intensity VIII. As a small increase in the level of macroseismic intensity from VII to VIII leads to much higher levels of damage, measures for risk management and seismic safety are necessary.

Through the mapping of the results, possible evacuation routes with different levels of accessibility were obtained. Blocked, restricted access and free roads were plotted considering both the façade walls prone to partial or total collapse and the narrowness of streets. The location of inaccessible areas is identified according to the width of the road, which influences the possibility of access to rescue vehicles, and the expected damage, which indicates the possible presence of debris in the road. Moreover, the number of isolated people who need to be rescued and the number of people that would circulate in the streets after the seismic event is an important part of the emergency planning. Identifying gathering points that are large enough to host all the people that can escape, and the location of isolated areas, are also essential in planning evacuation routes and rescue strategies. In this specific regard, it is worth adding that the capabilities of the this and similar seismic vulnerability assessment methods could also be used in simulation tools to better evaluate the effectiveness of choice in respect to the effective evacuation behaviors adopted by the residents, see for example [3]. The last important factor of the evacuation of the city center is the location of young and elderly people who should be rescued first.

Regarding the proposed retrofitting strategies, the size of inaccessible areas can be reduced. Almost all of the roads are accessible to pedestrians. The number of isolated people is zero, as the isolated areas correspond to unoccupied buildings, according to the data collected during fieldwork and that provided by the municipality of Leiria. As for the evacuation routes, even in the retrofitted scenario where the total number of people circulating in the streets after the seismic event is higher than in the non-retrofitted one, the available free areas to use as gathering points are large enough to host all of the evacuees. Further studies should be devoted to the evaluation of the effect of the retrofitting on the evacuation behaviors of the residents.

In conclusion, the vulnerability assessment method applied in this work is suitable for large-scale analysis for two reasons: it requires a small amount of information and fewer resources when compared to the robustness of the results, and the currently available simplified mechanical models to rapidly evaluate the seismic vulnerability of historic city centers still require experimental validation. Furthermore, it can be combined with additional assessment variables, such as the cost associated with the proposed retrofitting strategies or other social vulnerability aspects, to move towards a more comprehensive community resilience assessment. As a final comment, it is worth underlining that the comparison between the vulnerability index values and the observations made in the fieldwork proves the efficiency of the method. Moreover, the possibility of spatial presentation of results makes GIS a useful tool in support of mitigation strategies and management of seismic risk.

Acknowledgements

This work was enabled and funded by the Advanced Masters in Structural Analysis of Monuments and Historic Constructions (SAHC) at the University of Minho and by the Portuguese Foundation for Science and Technology (FCT) through the postdoctoral fellowship SFRH/BPD/122598/2016. The authors would like to thank the students at the Polytechnic Institute of Leiria for their assistance with coordinating and executing fieldwork. Additionally, many thanks to the Municipality of Leiria for providing access to their records and support of the work. A final acknowledgment is due to the two anonymous reviewers who, through their insightful comments, have contributed significantly to improve the overall quality of the work.

Appendix A. Supplementary data

Supplementary data to this article can be found online at https://doi.org/10.1016/j.ijdrr.2019.101432.

References

[1] J.L.P. Aguado, T.M. Ferreira, P.B. Lourenço, The use of a large-scale seismic vulnerability assessment approach for masonry façade walls as an effective tool for evaluating, managing and mitigating seismic risk in historical centers, Int. J. Archit. Herit. 12 (2018) 1259–1275, https://doi.org/10.1080/15583058.2018.1503366.

[2] J. Ortega, G. Vasconcelos, H. Rodrigues, M. Correia, A vulnerability index formulation for the seismic vulnerability assessment of vernacular architecture, Eng. Struct. 197 (2019), https://doi.org/10.1016/j.engstruct.2019.109381.

[3] A. Zlateski, M. Lucesoli, G. Bernardini, T.M. Ferreira, Integrating human behaviour and building vulnerability for the assessment and mitigation of seismic risk in historic centres: proposal of a holistic human-centred simulation-based approach, Int. J. Disaster Risk Reduc. 43 (2020), https://doi.org/10.1016/j.ijdrr.2019.101392.

[4] T.M. Ferreira, R. Maio, R. Vicente, Analysis of the impact of large scale seismic retrofitting strategies through the application of a vulnerability-based approach on traditional masonry buildings, Earthq. Eng. Eng. Vib. 16 (2017) 329–348, https://doi.org/10.1007/s11803-017-0385-x.

[5] R.R. Mili, K.A. Hosseini, Y.O. Izadkhah, Developing a holistic model for earthquake risk assessment and disaster management interventions in urban fabrics, Int. J. Disaster Risk Reduc. 27 (2018) 355–365, https://doi.org/10.1016/j.ijdrr.2017.10.022.

[6] S.R. Shrestha, R. Sliuzas, M. Kuffer, Open spaces and risk perception in post-earthquake Kathmandu city, Appl. Geogr. 93 (2018) 81–91, https://doi.org/10.1016/j.apgeog.2018.02.016. ISSN 0143-6228.

[7] N. Jaramillo, M.L. Carreño, N. Lantada, Evaluation of social context integrated into the study of seismic risk for urban areas, Int. J. Disaster Risk Reduc. 17 (2016) 185–198, https://doi.org/10.1016/j.ijdrr.2016.05.002.

[8] T.M. Ferreira, R. Vicente, H. Varum, Seismic vulnerability assessment of masonry facade walls: development, application and validation of a new scoring method, Struct. Eng. Mech. 50 (2014) 541–561, https://doi.org/10.12989/sem.2014.50.4.541.

[9] T.M. Ferreira, R. Maio, A.A. Costa, R. Vicente, Seismic Vulnerability Assessment of Stone Masonry Façade Walls: Calibration Using Fragility-Based Results and Observed Damage. Soil Dynamics and Earthquake Engineering, vol. 103, Elsevier, 2017, pp. 21–37, https://doi.org/10.1016/j.soildyn.2017.09.006. December 2017.

[10] S. Granda, T.M. Ferreira, Large-scale vulnerability and fire risk assessment of the historic centre of quito, Ecuador, Int. J. Archit. Herit. (2019), https://doi.org/10.1080/15583058.2019.1665142.

[11] T.M. Ferreira, R. Maio, R. Vicente, Seismic vulnerability assessment of the old city centre of Horta, Azores: calibration and application of a seismic vulnerability index method, Bull. Earthq. Eng. 15 (2017) 2879–2899, https://doi.org/10.1007/s10518-016-0071-9.

[12] QGIS, Development Team, QGIS Geographic Information System, Open Source Geospatial Foundation, 2019. http://qgis.osgeo.org.

[13] J. Mattoso, A cidade de Leiria na historia medieval de Portugal, Ler historia 4 (1985) 2–19 (in Portuguese).

[14] P. Teves-Costa, J. Batlló, L. Matias, C. Catita, M.J. Jiménez, M. García-Fernández, Maximum intensity maps (MIM) for Portugal mainland, J. Seismol. 23 (2019) 417–440, https://doi.org/10.1007/s10950-019-09814-5.

[15] S.A. Gomes, A Organizaçao do Espaço Urbano numa Cidade Estremenha: Leiria Medieval. *A Cidade, Jornadas Inter e Pluridisciplinares,* Actas II, Universidade Aberta, Lisboa, 1993, pp. 81–112 (in Portuguese).

[16] S.A. Gomes, Higiene e saúde na Leiria Medieval. Actas do III Coloquio sobre Historia de Leiria e da sua Região, 1999 (in Portuguese).
[17] GNDT, Manuale Per La Compilazione Della Scheda Gndt/Cnr Di Livello Ii Versione Modificata Dalla Regione Toscana, Regione Toscana, 2003 (in Italian).
[18] T. Gomes, Caracterização do Parque Edificado do Centro Histórico de Leiria, MSc Thesis, Polytechnic Institute of Leiria, 2016.
[19] T. Gomes, F. Gaspar, H. Rodrigues, Characterisation of Building Stock and its Pathologies: Case Study of the Historical City Centre of Leiria, Portugal. Nondestructive Techniques for the Assessment of Historic Structures, CRC Press, 2017, ISBN 9781138710474, pp. 21–38.
[20] A. Borri, M. Corradi, G. Castori, A. De Maria, A method for the analysis and classification of historic masonry, Bull. Earthq. Eng. 13 (2015) 2647–2665, https://doi.org/10.1007/s10518-015-9731-4.
[21] Circolare 21 gennaio 2019 n 7 C.S.LL.PP, Circolare 21 gennaio 2019 n. 7 C.S.LL.PP. Istruzioni per l'applicazione dell'aggiornamento delle "Norme Tecniche per le Costruzioni" di cui al D.M. 17/01/2018, 2008. Suppl. ord. alla G.U. n. 35 del 11/2/19.
[22] P. Pinheiro, P. Fernandes, P. Santos, H. Rodrigues, Mechanical Characterization of Masonry Walls with Flat-Jack Tests. Nondestructive Techniques for the Assessment of Historic Structures, CRC Press, 2017, ISBN 9781138710474, pp. 53–73.
[23] G. Grünthal, European Macroseismic Scale 1998 (EMS-98). Cahiers du Centre Européen de Géodynamique et de Séismologie, vol. 15, Centre Européen de Géodynamique et de Séismologie, Luxembourg, 1998.
[24] A. Bernardini, S. Giovinazzi, S. Lagomarsino, S. Parodi, Vulnerabilità e previsione di danno a scala territoriale secondo una metodologia macrosismica coerente con la scala EMS-98, 2007 (in Italian), https://ir.canterbury.ac.nz/handle/10092/4060.
[25] T.M. Ferreira, R. Vicente, J.A.R. Mendes da Silva, H. Varum, A. Costa, Seismic vulnerability assessment of historical urban centres: case study of the old city centre in Seixal, Portugal, Bull. Earthq. Eng. 11 (2013) 1753–1773, https://doi.org/10.1007/s10518-013-9447-2.
[26] R. Vicente, S. Parodi, S. Lagomarsino, H. Varum, J.A.R.M. Silva, Seismic vulnerability and risk assessment: case study of the historic city centre of Coimbra, Portugal, Bull. Earthq. Eng. 9 (2011) 1067–1096, https://doi.org/10.1007/s10518-010-9233-3.
[27] F. Bramerini, G. Di Pasquale, A. Orsini, A. Orsini, A. Pugliese, R. Romeo, F. Sabetta, Rischio sismico del territorio italiano. Proposta per una metodologia e risultati preliminari, Rapporto tecnico del Servizio Sismico Nazionale SSN. SSN/RT/95/01, Roma, 1995 (in Italian).
[28] S. Giovinazzi, The Vulnerability Assessment and the Damage Scenario in Seismic Risk Analysis, PhD Thesis, Technical University Carolo-Wilhelmina & University of Florence, 2005.
[29] S. Artese, V. Achilli, A GIS tool for the management of seismic emergencies in historical centers: how to choose the optimal routes for civil protection interventions, Int. Arch. Photogramm. Remote Sens. Spat. Inf. Sci. XLII-2/W11 (2019) 99–106, https://doi.org/10.5194/isprs-archives-XLII-2-W11-99-2019.
[30] S. Santarelli, G. Bernardini, E. Quagliarini, Earthquake building debris estimation in historic city centres: from real world data to experimental-based criteria, Int. J. Disaster Risk Reduc. 31 (2018) 281–291, https://doi.org/10.1016/j.ijdrr.2018.05.017.
[31] S. Argyroudis, J. Selva, P. Gehl, K. Pitilakis, Systemic seismic risk assessment of road networks considering interactions with the built environment, Comput. Aided Civ. Infrastruct. Eng. 30 (2015) 524–540, https://doi.org/10.1111/mice.12136.
[32] K. Ertugay, S. Argyroudis, H.S. Düzgün, Accessibility modeling in earthquake case considering road closure probabilities: a case study of health and shelter service accessibility in Thessaloniki, Greece, Int. J. Disaster Risk Reduc. 17 (2016) 49–66, https://doi.org/10.1016/j.ijdrr.2016.03.005.
[33] C. Dinis, *Estudo Sócio-Demográfico do Centro Histórico da Cidade de Leiria*, Departamento de Planeamento, Divisão da Habitação e Reabilitação Urbana, Câmara Municipal de Leiria, Leiria, 2006 (in Portuguese).